Energy transfer from photocarriers into the magnetic ion system mediated by a two-dimensional electron gas in (Cd,Mn)Te/(Cd,Mg)Te quantum wells

B. König
Physikalisches Institut der Universität Würzburg, D-97074 Würzburg, Germany

I. A. Merkulov
A. F. Ioffe Physical-Technical Institute, Russian Academy of Sciences, 194021 St. Petersburg, Russia

D. R. Yakovlev
Physikalisches Institut der Universität Würzburg, D-97074 Würzburg, Germany
and A. F. Ioffe Physical-Technical Institute, Russian Academy of Sciences, 194021 St. Petersburg, Russia

W. Ossau
Physikalisches Institut der Universität Würzburg, D-97074 Würzburg, Germany

S. M. Ryabchenko
Institute of Physics, National Academy of Sciences of Ukraine, 252650 Kiev, Ukraine

M. Kutrowski, T. Wojtowicz, G. Karczewski, and J. Kossut
Institute of Physics, Polish Academy of Sciences, 02-668 Warsaw, Poland
(Received 27 December 1999)

An efficient energy-transfer channel from photocarriers to the Mn spin system via a two-dimensional electron gas (2DEG) in *n*-type modulation-doped $Cd_{0.99}Mn_{0.01}Te/Cd_{0.76}Mg_{0.24}Te$ quantum wells has been found. The energy relaxation of photoexcited carriers is assumed to cause heating of the electron gas, which subsequently leads to an increase of the temperature of the Mn spin system. The mechanism of the energy transfer from the 2DEG to the Mn system involves a spin-flip scattering process originating in a strong electron-Mn exchange interaction. We have observed a suppression of the Mn heating with an increasing magnetic field which results in unusual energy shifts of the exciton, and trion features seen both in the photoluminescence and in reflectivity spectra. A theoretical model has been developed which is in a good agreement with experimental results. In the framework of this model we also analyze the details of the dependence of Mn-ion heating on the electron concentration and on the magnetic ion content.

I. INTRODUCTION

A variety of physical phenomena arises by incorporating magnetic atoms (e.g., Mn) in a semiconductor material. In these so-called diluted magnetic (or semimagnetic) semiconductors (DMS's) a strong *sp-d* exchange interaction between the conduction or valence electrons (or holes) and the magnetic ions is responsible for such large and spectacular effects as the ''giant'' Zeeman splitting of the band states and/or the formation of a magnetic polaron state.[1–3]

For a clear understanding of magnetic and optical properties of DMS's, it is necessary to consider the coupling (involving an exchange of the energy and of the magnetic moments) of all systems of the entire crystal, namely (i) the phonon system, (ii) the magnetic ion system, and (iii) the carriers. In particular, in the case of a semimagnetic quantum-well (QW) structure with an excess two-dimensional electron gas (2DEG), it is worthwhile to divide the carrier system further into photoexcited carriers and a pre-existing 2DEG already residing in the QW. The photocarriers, which are generated by light absorption, usually have an excess energy and a finite lifetime limited by various recombination processes. The 2DEG, on the other hand, originates from the modulation doping, and can be characterized by an infinite lifetime. These systems of modulation-doped QW's are shown schematically in Fig. 1. Each of them can be characterized by its heat capacity, (i.e., they are

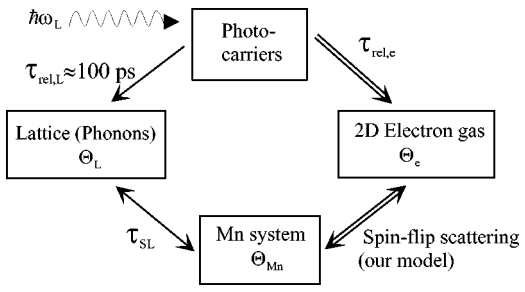

FIG. 1. Different energy reservoirs that participate in the Mn heating process for DMS heterostructures. Relaxation channels responsible for the heating of the Mn system are denoted by arrows. Photocarriers created by light of energy $\hbar\omega_L$ transfer their energy to the electron and to the phonon system. τ_{SL} denotes the spin-lattice relaxation time. The most effective channels for the energy transfer from the photocarriers to the Mn system are shown by double arrows.

energy reservoirs), its total magnetic moment, and its individual temperature Θ_i. Interactions between the systems result in an exchange of the energy and the magnetic moments. In this paper we limit ourselves to an examination of the energy transfer from the photocarriers into the system of Mn ions. The role of the 2DEG as an intermediate agent for this energy transfer will be at the center of our attention.

In Fig. 1 one can easily identify three possible routes for the energy transfer from the photocarriers into the magnetic system. First, there is a direct coupling of the photocarriers to the magnetic ions. Such a phenomenon has been investigated by means of photoluminescence,[4–7] by optically induced magnetization[8–10] and by optical orientation.[11] In those studies spin-flip exchange scattering was suggested as the most significant mechanism. However, the experimentally observed behaviors in Refs. 4–7 do not indicate conclusively that the direct interaction between photocarriers and magnetic ions does indeed have a very high efficiency.

The second possible route is one mediated by the phonon system. It requires the existence of an efficient coupling between the phonons and the magnetic system, which is, in fact the case for DMS's containing relatively large concentration of magnetic ions (more than 5%). In very dilute systems where Mn ions are isolated entities, the spin-lattice relaxation rate is extremely low. However, it may be increased by several orders of magnitude if clusters of magnetic ions are formed.[12,13] The effectiveness of the second route may also be limited at the stage of photocarrier coupling to the phonon system: the typical cooling time of electrons is about 2 ps for emission of optical phonons, and ranges widely from 1 to 100 ps for emission of acoustic phonons.[14]

Finally, there is a third route which is mediated by the 2DEG. It has been demonstrated that due to an efficient carrier-carrier interaction the photocarriers can transfer a considerable part of their kinetic energy to the 2DEG system instead to the phonon system.[15] Being accumulated in the 2DEG, this energy can be transferred further to the magnetic system. We have found no experimental information in the literature about the efficiency of this process of energy exchange between the 2DEG and the magnetic system. Our present experimental and theoretical efforts are aimed at shedding light on this problem.

For the present study we have chosen $Cd_{0.99}Mn_{0.01}Te/Cd_{0.76}Mg_{0.24}Te$ QW's with *n*-type modulation doping in the barrier layers. The choice of the system is motivated by several factors: (i) magneto-optical properties of (Cd,Mn)Te/(Cd,Mg)Te QW's have been widely studied during the last period[16,17]; (ii) modulation-doped II-VI QW's with a 2DEG have also been investigated[18,19]; (iii) the 2DEG concentration can be varied in these structures in a certain range by means of illumination; and (iv) a low Mn content $x_{Mn} \approx 0.01$ was chosen as a compromise between two conflicticting requirements: to minimize the efficiency of the interaction between the magnetic system and the phonons (that requires, in turn, to keep the Mn-content low) and, on the other hand, to have a pronounced giant Zeeman splitting of excitons, which is to be used as a tool in our studies.

Recently, an increased interest in DMS's was stirred up due to the prediction of a hole-gas-induced ferromagnetism[20] which was later experimentally confirmed in *p*-type doped (Cd,Mn)Te-based quantum wells by the observation of a zero-field splitting of the photoluminescence line below a critical temperature.[21] Here we demonstrate that the magnetization of a semimagnetic semiconductor can also be altered by the presence of an electron gas, though via an entirely different mechanism.

The paper is organized as follows: Section II details the sample design and the experimental setup. Section III describes the experiment data, and is followed by a survey on energy relaxation of photocarriers in semimagnetic semiconductors in Sec. IV. Section V presents the theoretical part. A discussion of the main results of our experiments and the theoretical considerations is given in Sec. VI, after which we summarize our findings.

II. EXPERIMENTAL DETAILS

The investigated sample was a $Cd_{0.99}Mn_{0.01}Te/Cd_{0.76}Mg_{0.24}Te$ quantum-well structure having a single QW 80 Å wide. It was fabricated by molecular-beam epitaxy on (100)-oriented GaAs substrates, covered by a 4.5-μm-thick CdTe buffer to improve the surface quality and the lattice matching with the barrier material. A ZnI_2 source has been used to dope a 19-Å-wide region of (Cd,Mg)Te:I which was separated by a 100-Å-thick spacer layer from the QW. The two-dimensional electron density was estimated to $n_e = 1.2 \times 10^{10}$ cm^{-2} by analyzing the exciton and trion oscillator strength observed in the reflectivity. The details of the procedure will be given in Sec. III.

Optical measurements were performed in pumped liquid helium at a temperature of 1.6 K. Magnetic fields up 7.5 T, generated by a superconducting split-coil solenoid, were applied parallel to the growth axis and to the direction of collected light (Faraday geometry). An Ar^+-ion laser operating at a wavelength of 514 nm served as an excitation source for the photoluminescence (PL) or as a pump source for a tunable dye laser (Pyridine 2) which was used for PL excitation (PLE) measurements. For reflectance experiments, a halogen lamp was used. The high-energy spectral range of the lamp emission was blocked by selective filters to avoid any heating of the sample. Due to optical selection rules for excitonic luminescence and absorption in the chosen geometry, the detected light was either right-hand (σ^+) or left-hand (σ^-) circularly polarized. The luminescence signal or the reflected light was dispersed by a 1-m monochromator and detected either with a charged-coupled device or a cooled photomultiplier, followed by a photon-counting system.

III. EXPERIMENTAL RESULTS

Figure 2 displays the luminescence spectra of our QW taken in the absence of a magnetic field. Due to the presence of free electrons in the QW, the PL signal (excitation energy $\hbar\omega_L = 2.41$ eV) exhibits a strong emission line at 1.6407 eV associated with negatively charged excitons X^- (trions), which are complexes consisting of two electrons bound to one hole,[19] and a rather weak emission due to uncharged heavy-hole excitons ($e1$-hh1,X) at a higher energy. The energy difference between X and X^- of 4 meV will be hereafter called the X^- binding energy. A small full width at half maximum (2.8 meV) of the X^- line, and its symmetric shape, point to a high structural quality of the investigated

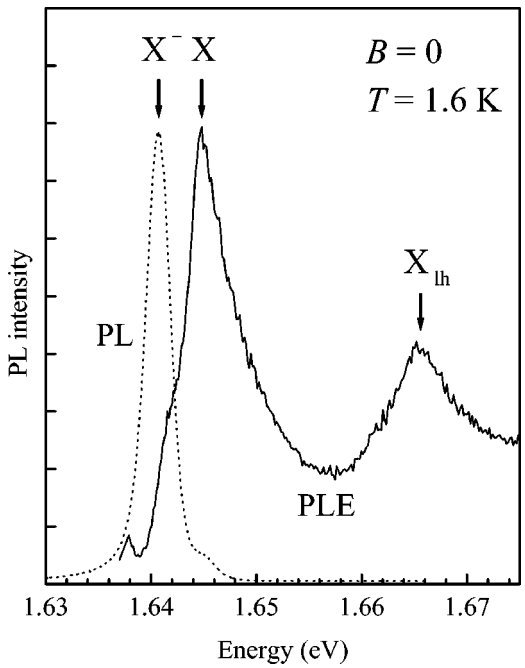

FIG. 2. Photoluminescence (dotted line) and PL excitation (solid line) spectra of a modulation-doped 80-Å-wide $Cd_{0.99}Mn_{0.01}Te/Cd_{0.76}Mg_{0.24}Te$ QW. Transitions related to the heavy-hole (X) and light-hole (X_{lh}) excitons and to the negatively charged exciton (X^-) are marked by arrows.

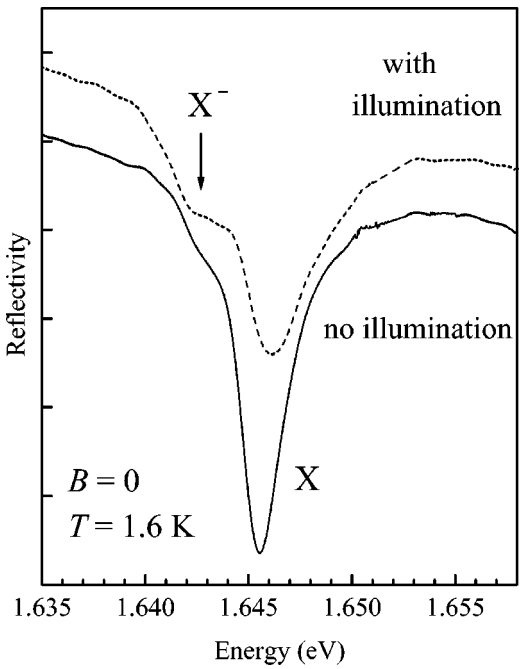

FIG. 3. The low-temperature reflectivity spectra of the modulation-doped 80-Å-wide $Cd_{0.99}Mn_{0.01}Te/Cd_{0.76}Mg_{0.24}Te$ QW detected at $B=0$ with (dashed curve) and without (solid curve) additional laser illumination of energy 2.41 eV, and at a power density 4 W/cm^2. The spectra are moved vertically for clarity.

sample. The PLE spectrum, which has been detected on the low-energy side of the X^- line at 1.637 eV, shows the feature due to absorption of X at 1.645 eV and of the light-hole exciton ($e1$-lh 1,X_{lh}) at 1.666 eV. The negligible Stokes shift of the X line proves a suppressed spectral diffusion for excitons in this structure. In contrast to the PL data, the negatively charged exciton contributes only very weakly to the absorption, and shows up in the PLE spectrum as a low-energy shoulder on the X signal. This behavior directly reflects the smaller density of states of X^- as compared to that of the neutral excitons.

Reflectivity spectra of the sample taken at $B=0$ and $T=1.6$ K under various additional illumination conditions are presented in Fig. 3. The reflectance signal recorded without laser illumination (solid line) is dominated by the X resonance, with the negatively charged exciton feature having a small oscillator strength, a situation which is similar to the observation in PLE. A considerable change of the spectrum occurs if the sample is additionally illuminated by the laser light with $\hbar\omega_L=2.41$ eV (which exceeds the barrier band gap E_B by about 0.4 eV). Since the laser beam was completely defocused to achieve a homogenous illumination, we can only estimate the power density to be about 4 W/cm^2. The resulting reflectivity (dashed line in Fig. 3), obtained by subtracting the laser-induced PL signal, reveals the following modifications: (i) the X^- resonance becomes more pronounced, and (ii) the illumination causes a broadening of the exciton resonance whose (iii) amplitude is also reduced. The intensity gain of the negatively charged exciton can be directly attributed to an increased electron concentration in the QW. This was previously also observed in (Zn,Mn)Se-based heterostructures, and explained there in terms of different mobilities of photoexcited carriers in the barrier which leads to a higher collection efficiency into the QW in the case of electrons.[22] To make a quantitative statement about the electron concentration and its increase by the illumination, we have simulated the reflectance spectra using the transfer matrix method[23] and a classical oscillator model for the dielectric function for both X and X^-. In this way the ratio r of the X to X^- oscillator strength was deduced to be $r=14.9$ or, in the case of illuminated sample, $r=5.6$ (the oscillator strength of the X resonance was kept constant). Following the procedure also used for ZnSe-based QW's (see Refs. 24 and 25) we determined $n_e=9\times10^{10}$ cm^{-2} and $r=2$ for a nonmagnetic CdTe/(Cd,Mg)Te QW. As r was shown in Ref. 24 to scale linearly with the electron density, for the studied structure we obtain $n_e=3.2\times10^{10}$ and 1.2×10^{10} cm^{-2} for conditions with and without laser illumination, respectively. Simultaneously with an increase of the electron density the exciton damping, determined by the calculation, is increased by a factor of 1.7. We attribute this additional broadening to a higher probability of the exciton scattering by free electrons.[26]

Due to the sp-d exchange interaction between the carriers and the Mn system, the reflectance signal splits into two branches when an external magnetic field is applied, as shown in Fig. 4(a) for $B=0.5$ T. With respect to the zero-field data (the X position at $B=0$ is marked by a thick vertical line) the exciton resonances are shifted by 4.5 meV to lower (higher) energy for σ^+ (σ^-) polarization. As a consequence of the electron-gas spin polarization and of the electron singlet nature of the trion state, the X^- resonance is completely suppressed in the σ^+-polarized spectrum similar to the behavior of neutral donor-bound excitons reported in Ref. 27. An illumination of the sample with the laser light having identical energy and power to that used in the zero-

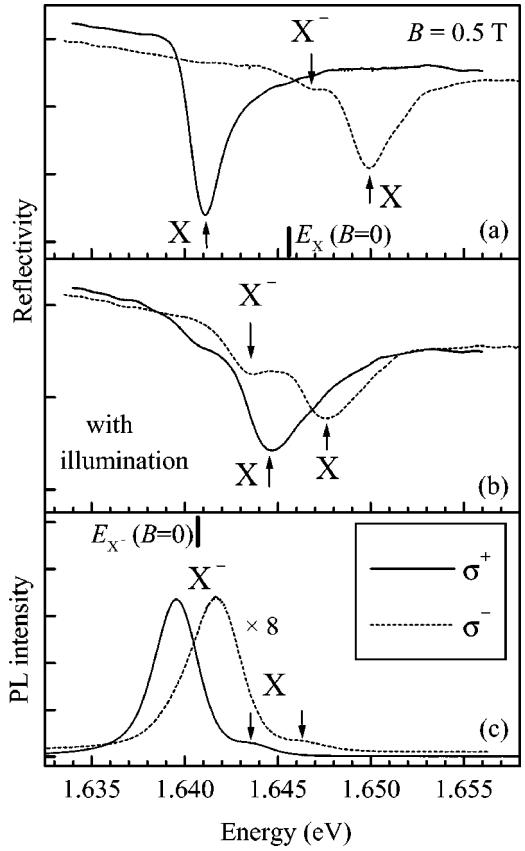

FIG. 4. (a) Reflectivity spectra of the modulation-doped 80-Å-wide $Cd_{0.99}Mn_{0.01}Te/Cd_{0.76}Mg_{0.24}Te$ QW at $B=0.5$ T and $T=1.6$ K, showing resonances due to neutral (X) and negatively charged (X^-) excitons. The spectra in panel (b) were recorded under additional laser illumination using light energy $\hbar\omega_L=2.41$ eV and power density $P_L=4$ W/cm^2. (c) The luminescence signal induced by a laser illumination of the same energy and power as used for the spectra in panel (b). Thick vertical lines mark the respective energy positions at zero field.

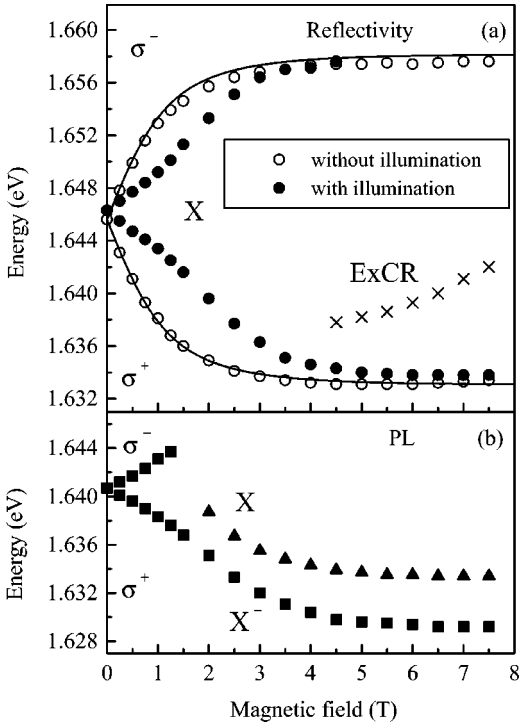

FIG. 5. The magnetic-field dependence of the exciton (X) and the trion (X^-) energies in the reflectivity [panel (a)] taken with (full symbols) and without laser illumination (open symbols) for a modulation-doped $Cd_{0.99}Mn_{0.01}Te/Cd_{0.76}Mg_{0.24}Te$ n-type QW. Panel (b) shows PL data. The solid lines represent calculations according to Eq. (1), with $x_{Mn}=0.01$ and $\Theta_{Mn}=1.6$ K.

field measurements (see Fig. 3) results in the reflectivity spectra presented in Fig. 4(b). Again, these reveal an exciton line broadening and a gain of the intensity of the X^- resonance. However, the most notable result of the illumination is a reduction of the exciton Zeeman splitting by about 80%. Note that the X^- oscillator strength changes can be compared only in the σ^--polarized spectra, as the intensity of the X^- feature in the σ^+-polarization depends on the electron concentration and on the electron-spin splitting which are *both* effected by the illumination with the laser. The luminescence spectra detected under the same conditions with the lamp beam blocked are plotted in Fig. 4(c). Similar to the laser-modified reflectance, the Zeeman splitting of X and X^- lines in PL is strongly suppressed as compared to reflectivity without above-barrier illumination.

From a series of measurements at different magnetic fields we deduced the X and X^- peak positions from the reflectivity and from the PL. We summarize these results in Figs. 5(a) and 5(b). An additional feature which can be resolved in the reflectance spectra for the magnetic fields $B>4.5$ T, and which shifts linearly with B, is identified as the combined exciton cyclotron resonance.[18] In the mean-field approximation, the energy of QW excitons with the total spin ± 1 varies because of sp-d interaction, and is described by (after Ref. 28)

$$E_X^{\pm 1}(B)=E_X(B=0)\pm\frac{1}{2}(\delta_e\alpha-\delta_h\beta)N_0x_{Mn}\langle S_z\rangle, \quad (1)$$

where $N_0\alpha=220$ meV and $N_0\beta=-880$ meV (Ref. 28) are the exchange constants for the conduction and valence bands, respectively, in (Cd,Mn)Te. N_0 is the inverse unit-cell volume, and x_{Mn} (in our case $x_{Mn}=0.01$) is the Mn mole fraction. Equation (1) in its original form for bulk DMS's has $\delta_e\equiv\delta_h\equiv 1$. In the case of low-dimensional systems, letting $\delta_{e(h)}\leqslant 1$ accounts for a reduced exchange interaction due to the leakage of the electron and hole wave functions into the nonmagnetic barriers in the case of (Cd,Mn)Te/(Cd,Mg)Te QW's. $\langle S_z\rangle$ represents the thermal average value of the Mn spin in the direction of the magnetic field $B=B_z$ at a Mn spin temperature Θ_{Mn}. It is expressed by the modified Brillouin function $B_{5/2}$ (Ref. 28)

$$\langle S_z\rangle=-S_{\rm eff}B_{5/2}\left[\frac{5g_{Mn}\mu_B B}{2k_B(\Theta_{Mn}+\Theta_0)}\right]. \quad (2)$$

Here $S_{\rm eff}$ and Θ_0 are the parameters for the effective Mn spin and temperature that phenomenologically describe the effect of the antiferromagnetic Mn-Mn exchange interaction. $g_{Mn}=2$ is the g factor of the Mn d state. Using Eq. (1) to model the energy shift of the exciton resonance by the magnetic field observed in the reflectivity without illumination yields $\Theta_{Mn}=1.6$ K, for the Mn temperature in agreement with the

sample bath temperature [see the solid lines in Fig. 5(a)]. In our calculations we used the values $E_X(B=0)=1.6456$ eV and $\delta_e=\delta_h=0.98$, which have been calculated from the electron and hole envelope function with valence-band offset $Q_V=0.41$.[29] $S_{\text{eff}}=2.15$, and $\Theta_0=0.44$ K, are both taken from Ref. 30 as for the bulk samples.

The most striking feature in Fig. 5(a) is an anomalously small energy shift of the exciton energy in small magnetic fields, clearly seen in the reflectance spectra under illumination. It is corroborated by the shift of the PL peak positions for the X and X^- signals [see Fig. 5(b)]. The suppression of the Zeeman splitting is about 60% at $B=1.5$ T and it decreases, and finally diminishes, with the field increasing. It is unlikely that any of the parameters, apart from Θ_{Mn}, appearing in Eqs. (1) and (2) can be modified by the photocarriers. Therefore, we explain the illumination-induced changes of E_X by a heating of the Mn system, i.e., by an increase of Θ_{Mn}. Moreover, the magnetic-field dependence of the exciton energy cannot be reproduced by Eq. (1) using any constant value of the Mn spin temperature. This leads us to the conclusion that the Mn heating is caused by the electron gas and not by direct interaction with photocarriers. In the case of a direct interaction between photocarriers and Mn ions, a circular polarization of the laser light should alter the heating of the Mn system by photoinduced (de)magnetization. However, no such influence of the laser polarization was found. That indicates the direct interaction of photocarriers with the Mn ions to be negligible for the studied structure. Our model of the heating mechanism is based on the spin-flip exchange scattering of the 2DEG by Mn ions, and will be presented in Sec. V.

One can see in Fig. 5 that the illumination-induced changes of the exciton energy are very similar in the reflectivity and in the luminescence spectra. Also similaritites exist when comparing the splitting of the exciton and trion features. Therefore, in our discussion of the laser power dependence of the shift we shall restrict ourselves to the σ^+-polarized X^- line observed in PL experiments. The peak position of the X^- luminescence excited with $\hbar\omega_L=2.41$ eV and having different laser powers P_L are displayed in Fig. 6 as a function of the magnetic field. The field-induced shift of the X^- energy is continuously suppressed when P_L increases even for moderate excitation powers typically used in PL experiments. The amplitude of this suppression is at maximum in the field range 1.5–3 T. The dotted line in Fig. 6 represents a calculation of E_X using Eq. (1) with $\Theta_{\text{Mn}}=1.9$ K, and $E_{X^-}(B=0)=1.6407$ eV, and with all remaining parameters fixed and equal to the values given above. A satisfactory agreement with the experimental data obtained for the lowest excitation power implies an absence of Mn heating by the electron gas for $P_L \leqslant 0.1$ W/cm^2. We suppose that a slight discrepancy of the Mn temperature (0.3 K) extracted from the PL and the reflectivity to be explained by a heating of the lattice in the case of the PL experiments (see discussion below). To describe the energy shift of the X^- line at higher P_L in the frame of Eq. 6 we have to assume that Θ_{Mn} is a function of the magnetic field. We have found that our experimental results could be described using the empirical formula

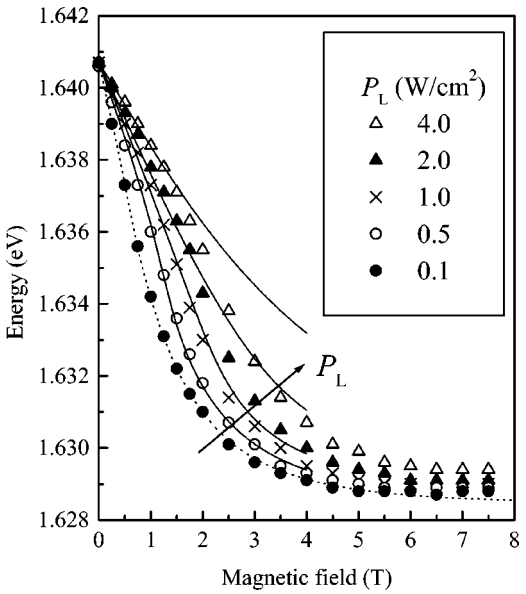

FIG. 6. The energy shift of the X^--line in a σ^+-polarized PL spectrum determined for different laser excitation powers P_L (laser energy $\hbar\omega_L=2.41$ eV). Theoretical data from Eq. (1) with $\Theta_{\text{Mn}}=1.9$ K are shown by the dashed line. The solid lines represent calculations using Eq. (1) with the magnetic-field dependence of Θ_{Mn} according to Eqs. (23) and (24).

$$\Theta_{\text{Mn}}(B)=\Theta_a+\Theta_b\exp\left(-\frac{B^2}{\gamma}\right), \quad \gamma>0, \tag{3}$$

with Table I giving the numerical values for the parameters Θ_a, Θ_b, and γ for different excitation powers P_L. They have been determined by fitting the exciton line shift with Eqs. (1) and (2), and modeling the Mn temperature Θ_{Mn} by Eq. (3). However, for the sake of precision we also determined $\Theta_{\text{Mn}}(B)$ directly by varying Θ_{Mn} at each magnetic field to fit exactly the experimental energy values. The magnetic-field dependence of the Mn temperature obtained in this way is depicted in Fig. 7 for various excitation powers P_L. At low fields Θ_{Mn} is considerably enhanced by up to about 8 K ($P_L=4$ W/cm^2), and then it drops to saturate for $B>4$ T.

Qualitatively the same unusual shift of the exciton and the trion energy was also present in a whole series of modulation-doped samples of a similar design (low Mn concentration $\approx 1\%$) confirming that we are not dealing with a

TABLE I. Parameters Θ_a, Θ_b, and γ appearing in Eq. (3), corresponding to experimental results presented in Fig. 6; n_e is the electron density for the excitation above the band gap of the barrier. The values for $P_L=0$ were obtained from the reflectivity measurements.

P_L (W/cm^2)	n_e(10^{10} cm^{-2})	Θ_a (K)	Θ_b (K)	γ (T^2)
0	1.2	1.65	–	–
0.1	1.3	1.85	–	–
0.5	1.5	2.17	1.72	2.64
1.0	1.7	2.47	3.04	3.37
2.0	2.2	3.12	4.25	4.22
4.0	3.2	3.84	4.88	5.19

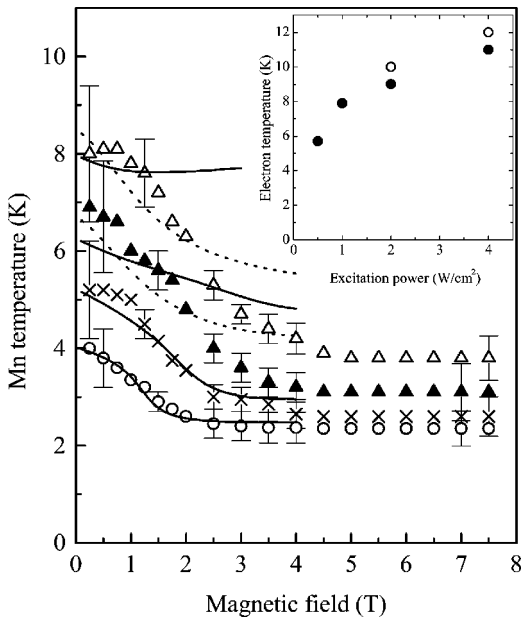

FIG. 7. Experimental (symbols) and theoretical values (solid lines) of the Mn temperatures Θ_{Mn} [after Eqs. (23) and (24)] as a function of the magnetic field for various excitation powers P_L. The dotted curves represent calculations, where a field dependence of the electron-spin relaxation time τ_s was allowed. Different symbols correspond to the same excitation powers as in Fig. 6. Inset: The electron temperature as a function of the laser excitation power (solid symbols) determined using Eqs. (23) and (24). Parameters used for $\tau_s(B)$ are shown by the open symbols.

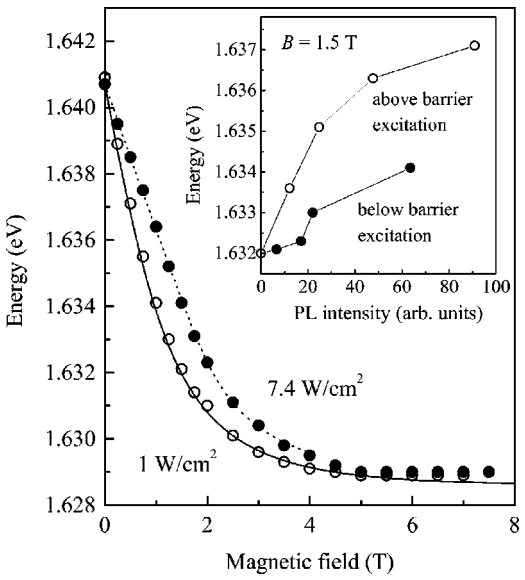

FIG. 8. The magnetic-field dependence of the σ^+-polarized X^- luminescence line excited with the laser energy $\hbar\omega_L = 1.75$ eV, which is below the band gap of the barrier and for different excitation power densities P_L. The curves represent calculations applying $\Theta_{\mathrm{Mn}} = 1.9$ K = const (solid line), and Θ_{Mn} determined by Eqs. (23) and (24) with $\Theta_L = 1.9$ K, $\Theta_e = 8.7$ K, and $\tau_s = 0.1$ ns (dashed line). Inset: X^--luminescence energy in the σ^+ polarization at $B = 1.5$ T as a function of the integral PL intensity for the below- (solid symbols) and above-the-barrier energy (closed symbols) excitation.

peculiarity of just one single sample. In particular, all samples revealed a pronounced reduction of the Zeeman splitting at moderate excitation densities and a vanishing of this effect with increasing magnetic field.

So far in this paper we have discussed the heating effect only for the above-barrier excitation. In such case, i.e., when $\hbar\omega_L > E_B$, an increase of P_L can affect two parameters: (i) it increases the number of the photocarriers collected (or excited directly) in the QW and, as a consequence, it increases the flux of energy transmitted from the photocarriers to the 2DEG, and (ii) it increases the concentration of the electron gas in the QW (an evidence of the latter effect are presented in Figs. 3 and 4). In order to separate these two contributions we performed also experiments using the below-barrier excitation condition ($\hbar\omega_L < E_B$) for which the 2DEG density is constant and equal to $n_e = 1.2\times10^{10}$ cm^{-2}. First, in Fig. 8 we show the magnetic-field dependence of the X^- luminescence energy (in σ^+ polarization) for two different excitation power densities and for the laser energy $\hbar\omega_L < E_B$. To ensure a constant absorption in the QW $\hbar\omega_L = 1.75$ eV was chosen since then the absorption spectrum (measured by PLE) is nearly magnetic field independent. For a low excitation power, $P_L = 1$ W/cm^2, the X^- line shift is described well using a constant $\Theta_{\mathrm{Mn}} = 1.9$ K (solid line in Fig. 8). However, in agreement with the studies of Sec. II, at a higher excitation power, $P_L = 7.4$ W/cm^2, fixed values of Θ_{Mn} cannot describe the observed dependecies correctly. This indicates that we again have a heating of the Mn system by the electron gas.

Here a problem appears of a comparison of the results for below- and above-barrier excitation. It is not proper to compare experimental results for the same value of P_L, because the number of generated electron-hole pairs differs strongly for the two cases, due to the energy dependence of the absorption coefficient. Moreover, the efficiency of the carrier collection from the barriers by the QW is not well known for the studied structure. Therefore, we have based our comparison on the assumption that only the carriers generated or collected in the QW contribute to the heating of the electron gas. In order to proceed, we assumed that here the PL intensity represents a meaningful parameter, since it is proportional to the number of electron-hole pairs recombining in the QW. In the inset to Fig. 8, the energy shift of the X^- line, which can be directly linked to Θ_{Mn}, is compared for the excitation above- (open symbols) and below-the-barrier (closed symbols) band gaps at $B = 1.5$ T as functions of the integral luminescence intensitiy (to obtain the same PL intensity, the laser power for below-the-barrier excitation has to be about twice as high as that for above-the-barrier excitation). In contrast to the case of $\hbar\omega_L < E_B$, for which the electron density is $n_e = 1.2\times10^{10}$ cm^{-2} and is independent of the excitation power (i.e., of the PL intensity), a more pronounced blueshift of the X^- line (i.e., an increase of Θ_{Mn}) is observed for $\hbar\omega_L > E_B$. In the latter case, the electron density increases with P_L up to $n_e = 3.2\times10^{10}$ cm^{-2}. Obviously the different energetic changes of the X^- line for the below- and above-the-barrier excitation can be ascribed to a dependence of the Mn temperature on n_e.

IV. ENERGY RELAXATION OF PHOTOCARRIERS IN SEMIMAGNETIC SEMICONDUCTORS

Before proceeding with a detailed theoretical analysis of the electron-induced Mn heating, let us first make an over-

view of different energy reservoirs and relaxation channels that, conceivably, may be of importance in the heating process (see Fig. 1). Initially, the created photocarriers have a certain amount of kinetic energy. The energy, as well as the concentration of the photocarriers themselves, are functions of the light intensity, of the absorption coefficient, and of the energy of the exciting laser $\hbar\omega_L$. Within a certain time $\tau_{\mathrm{rel},L}$, which in the case of emission of acoustic phonons, ranges from 1 to about 100 ps, the photocarriers relax their energy. It is passed to the lattice and results in raising of the lattice temperature Θ_L. In addition, the Coulomb interaction makes possible the energy transfer from the photocarrier to the electron gas[31] (time constant $\tau_{\mathrm{rel},e}$). It was recently shown that this relaxation channel may be more efficient than the phonon emission.[15] We shall assume that it is also so in our case. The temperature of the electron gas is determined mainly by the energy tranferred from the photocarriers, and by the energy flux from the electron gas to the lattice.

A heating of the magnetic system directly by photocarriers was shown experimentally to be important in the presence of a high-density electron-hole (e-h) plasma leading to the formation of domains in the magnetic system with low and high temperatures.[6] As the e-h plasma transforms into a system of excitons, the heating of Mn system was shown to vanish. This may be attributed to a combined spin-flip processes of the electrons and holes within the exciton complex,[32,33] with a decreasing spin-flip scattering rate on Mn ions. Ryabchenko *et al.*[7] studied the Mn heating by the photocarriers in $Cd_{0.95}Mn_{0.05}Te$ bulk crystals, using time-integrated PL, excitation densities up to 10 W/cm^2, and magnetic fields $B \leqslant 2$ T. From their data we estimated an increase of the Mn temperature by ≈ 0.6 K for $B=1.5$ T and at $P_L=4$ W/cm^2, which is equal to the maximum power density used in the present work for above-barrier excitation. Such degree of the Mn heating is about ten times smaller than that observed for our structure (cf. Fig. 7). Further, in Ref. 7, a nonmonotonic behavior of the Mn temperature on P_L at low magnetic fields ($B<1.5$ T) was reported with an initial decrease for power densities up to ≈ 2.5 W/cm^2, and then followed by an onset of an increase with P_L. This result was explained by the exchange scattering of holes by the Mn ions, which gives rise to an effective magnetization of the Mn system, i.e., to a decrease of Θ_{Mn} (also see Ref. 34). In contrast to these results, we have observed a monotonic heating of the Mn system with an increasing power density for a constant magnetic field. Thus, in view of the moderate excitation powers used in our experiments, which are to small to generate an e-h plasma, and in view of the basic differences with the results of Ref. 7, it is justified to neglect the direct interaction between the photocarriers and Mn ions. The heating of the Mn system is ascribed by us to be an effect of the presence of the electron gas.

The spin-lattice relaxation of Mn ions with a rate $1/\tau_{\mathrm{SL}}$ drives the magnetic system to thermal equilibrium with the lattice. It has been reported that in (Cd,Mn)Te τ_{SL} decreases with increasing Mn content by several orders of magnitude as the relaxation is predominantly mediated by clusters of ions[12,13] (e.g., for $x_{\mathrm{Mn}}=0.01$, $\tau_{\mathrm{SL}}\approx 10^{-5}$ s, and for $x_{\mathrm{Mn}}=0.05$, $\tau_{\mathrm{SL}}\approx 10^{-7}$ s). Therefore, only a small Mn content permits one to observe a Mn heating by the 2DEG, as mentioned in our motivation of the choice of the samples. Under steady-state conditions each system of DMS QW's (see Fig. 1) is defined by its individual temperature. For our structure we do not have quantitative information about the interaction between the photocarriers and the 2DEG. Therefore, we shall regard the temperature of the electron gas as an adjustable parameter in the analysis presented in Sec. VI.

The exchange interaction has often been theoretically considered in the past to calculate the relaxation rate of the carriers by magnetic impurities (e.g., see Refs. 35, 36, and 37). Unfortunately, none of these papers addressed this problem in the context of Mn system heating.

V. THEORY

Here we present details of our theoretical model for the field-dependent heating of the Mn system mediated by a 2DEG. The value of the Mn spin temperature is determined by the balance between the heating by the 2DEG and cooling by spin-lattice interaction:

$$\left.\frac{dE}{dt}=\frac{\partial E}{\partial t}\right|_{e\text{-Mn}}+\left.\frac{\partial E}{\partial t}\right|_{\text{Mn-lat}}=0. \tag{4}$$

In a phenomenological model the term for the spin-lattice relaxation reads

$$\left.\frac{\partial E}{\partial t}\right|_{\text{Mn-lat}}\approx-\frac{E(B,\beta_{\mathrm{Mn}})-E(B,\beta_L)}{\tau_{\mathrm{SL}}}=N\xi^2\frac{\beta_{\mathrm{Mn}}-\beta_L}{T_{\mathrm{SL}}(B,\beta_L,\beta_{\mathrm{Mn}})} \tag{5}$$

where $\beta_{\mathrm{Mn}}=(k_B\Theta_{\mathrm{Mn}})^{-1}$ and $\beta_L=(k_B\Theta_L)^{-1}$ are the inverse temperature of the magnetic ions and the inverse lattice temperature, and $E(B,\beta)=N\xi I_1(\xi\beta)$ is the energy of the Mn spin system. $\xi=\mu_B g_{\mathrm{Mn}}B$ is the Zeeman splitting of Mn spin levels in an external magnetic field B, μ_B is the Bohr magneton, and $g_{\mathrm{Mn}}=2$ is the g factor of the Mn d state. N is the total number of Mn ions, $I_1(\xi\beta)$ is the average value of the Mn spin, τ_{SL} is the characteristic time of the spin-lattice relaxation, and $T_{\mathrm{SL}}\equiv\tau_{\mathrm{SL}}\xi(\beta_L-\beta_{\mathrm{Mn}})/[I_1(\xi\beta_L)-I_1(\xi\beta_{\mathrm{Mn}})]$. From Eqs. (4) and (5), we obtain the increase of the Mn spin temperature caused by interaction with a 2DEG:

$$\beta_{\mathrm{Mn}}-\beta_L=-\frac{T_{\mathrm{SL}}}{N\xi^2}\left.\frac{\partial E}{\partial t}\right|_{e\text{-Mn}}. \tag{6}$$

The overheating of the Mn system by the 2DEG is mediated by a spin-flip process which changes the number N_M of Mn ions in the state $M(=-5/2,-3/2,\ldots,3/2,5/2)$ and, consequently, influences the Mn spin temperature:

$$\left.\frac{\partial E}{\partial t}\right|_{e\text{-Mn}}=\xi\sum_M M\frac{\partial N_M}{\partial t}. \tag{7}$$

For calculating $\partial N_M/\partial t$ we start with the well-known Hamiltonian for the s-d exchange interaction between the conduction electrons (a wave function of s-like symmetry) and the d shell of Mn ions:

$$H_{\mathrm{exch}}=\frac{1}{2}\alpha\sum_i \boldsymbol{\sigma}\mathbf{S}_i\delta(\mathbf{r}-\mathbf{R}_i)=\sum_i H_{\mathrm{exch},i}. \tag{8}$$

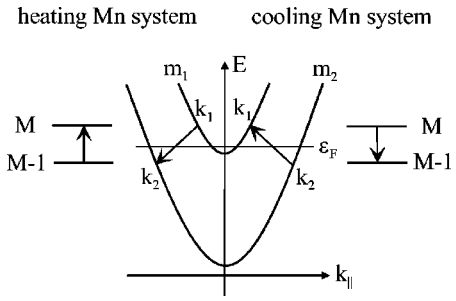

FIG. 9. Schematic energy levels of the electron $(m_i,\mathbf{k}_i)$ and Mn system (M) that contribute to the spin-flip scattering process. Left hand: increase of the Mn spin temperature; right hand: decrease of the Mn spin temperature. The Fermi energy is denoted by ε_F.

$\mathbf{r}$ and $\mathbf{R}_i$ are the coordinates of the electron and the ith magnetic ion, respectively. α is the exchange constant, $\boldsymbol{\sigma}$ is the vector of the spin Pauli matrixes, and $\mathbf{S}_i$ is the spin operator of the Mn ion. Applying Fermi's golden rule for the case of an energy conserving spin-flip process, the time evolution of N_M reads

$$\frac{\partial N_M}{\partial t}=\frac{2\pi}{N\hbar}\frac{S^2}{(2\pi)^4}\sum_{\substack{m_1,m_2,\\ M',i}}\int\int d^2k_1 d^2k_2[N_{M'}f_{m_1,\mathbf{k}_1}\times(1-f_{m_2,\mathbf{k}_2})-N_M f_{m_2,\mathbf{k}_2}(1-f_{m_1,\mathbf{k}_1})]\big|\times\langle m_1,\mathbf{k}_1,M'|H_{\mathrm{exch},i}|m_2,\mathbf{k}_2,M\rangle|^2\times\delta(E_M-E_{M'}-\varepsilon_{m_1,\mathbf{k}_1}+\varepsilon_{m_2,\mathbf{k}_2}), \tag{9}$$

where $M'=M\pm1$, $m_1=\mp1/2$, and $m_2=\pm1/2$. S is the sample area, $\varepsilon_{m_l,\mathbf{k}_l}=\varepsilon_{\mathrm{kin},l}+\varepsilon_{m_l}$ denotes the total (kinetic and spin) energy of electrons with momentum $\mathbf{k}_l$ and a z projection of spin m_l, and $E_M=\xi M$ is the energy of the Mn d shell in state M. For the electron Fermi-Dirac distribution function $f_{m,\mathbf{k}}=[\exp(\varepsilon_{m,\mathbf{k}}-\varepsilon_{F,m})+1]^{-1}$, we introduced individual Fermi levels $\varepsilon_{F,m}$ for spin subbands with $m=+1/2$ and $-1/2$. We note here that the electron momentum on the Fermi level is $k_F=[2m_e(\varepsilon_{F,m_l}-\varepsilon_{m_l})/\hbar]^{1/2}$, where m_e is the electron effective mass. In thermodynamic equilibrium the electron temperature is equal to the lattice temperature, and $\varepsilon_{F,1/2}=\varepsilon_{F,-1/2}=\varepsilon_F$. In this case the spin polarization depends only on the electron spin splitting $\varepsilon=\varepsilon_{1/2}-\varepsilon_{-1/2}$. The flipflop collision with magnetic ions repopulates the electron-spin subbands, and creates a difference between their Fermi levels: $\Delta\varepsilon_F=\varepsilon_{F,+1/2}-\varepsilon_{F,-1/2}$.

To illustrate the scattering process, Fig. 9 shows a scheme of the participating electron and Mn levels. An electron in the state $|m_i,\mathbf{k}_i\rangle$ is scattered via the nondiagonal elements of the exchange Hamiltonian (8) into a state $|m_j,\mathbf{k}_j\rangle$. The energy difference of these two states from the Zeeman splitting of the Mn ion spin sublevels is E_M-E_{M-1}. If the electron's initial spin is m_1, a Mn ion with $J_z=M'=M-1$ is excited into the state M, which is equivalent to an increase of the Mn spin temperature (the left-hand side of the figure). The reversed process leads to a cooling of the magnetic ion system, as shown on the right-hand side of Fig. 9. The probabilities for the two processes are functions of the electron and Mn spin splitting. The electron momentum is changed in the scattering process by $\mathbf{k}_j-\mathbf{k}_i$. This momentum difference is taken from or absorbed by the lattice with the Mn ion as the mediating particle.

Since there is a strong confinement in the z direction, only electron states from the first quantum-confined subband are taken into account. In the case of the QW studied here only 2% of the electron wave function penetrates the barriers [$\delta_e=0.98$, see Eq. (2)]. Therefore, we may approximate the electron envelope function by that of a QW with the infinite barriers. Thus the electron eigenfunction reads

$$\Psi_e=\sqrt{\frac{2}{SL}}\exp(i\mathbf{k}_\parallel\mathbf{r})\cos(k_z z)|m_l\rangle,\quad l=1\ \text{ and }\ 2, \tag{10}$$

with L being the quantum-well width and $\mathbf{k}_\parallel$ the electron momentum in the QW plane. The matrix element in Eq. (9) is then obtained in the form

$$|\langle-1/2,\mathbf{k}_1,M|H_{\mathrm{exch},i}|+1/2,\mathbf{k}_2,M-1\rangle|^2=\frac{\alpha^2}{(SL)^2}\cos^4(k_z z_i)\left(\frac{5}{2}+M\right)\left(\frac{5}{2}-M+1\right). \tag{11}$$

The summation over all Mn ions is performed by averaging over the QW volume V accounting for the probability to find a Mn ion (x_{Mn} is the Mn mole fraction):

$$\sum_i\cos^4(k_z z_i)\to x_{\mathrm{Mn}}N_0\int_V\cos^4(k_z z_i)dV=\frac{3}{8}N. \tag{12}$$

By inserting Eqs. (11) and (9) into Eq. (7), we finally obtain an expression for the energy flux from the 2DEG to the magnetic ion system,

$$\left.\frac{\partial E}{\partial t}\right|_{e\text{-Mn}}=\frac{2\xi N}{T_{e\text{-Mn}}}\sinh\left[\frac{\xi(\beta_{\mathrm{Mn}}-\beta_e)+\Delta\varepsilon_F\beta_e}{2}\right]\approx\frac{\xi^2 N}{T_{e\text{-Mn}}}\left(\beta_{\mathrm{Mn}}-\beta_e+\frac{\Delta\varepsilon_F\beta_e}{\xi}\right), \tag{13}$$

where

$$T_{e\text{-Mn}}=\frac{2}{W(\varepsilon,\Delta\varepsilon_F,\xi,\beta_e)F(\xi\beta_{\mathrm{Mn}})} \tag{14}$$

is a characteristic time for the electron-Mn relaxation process. The functions W and F are defined as

$$W=\frac{3\alpha^2 m_e^2 \exp[(\xi-\Delta\varepsilon_F)\beta_e/2]}{4\pi\hbar^5 L^2}\int_{\varepsilon/2}^{\infty} dE f_{1/2}(E)[1-f_{-1/2}(E-\Delta\varepsilon_F)]$$

$$=\frac{3\alpha^2 m_e^2}{8\hbar^5 L^2 \pi\beta_e \sinh[(\xi-\Delta\varepsilon_F)\beta_e/2]}\left\{\ln\frac{\cosh[(2\varepsilon_F-\varepsilon+2\xi-\Delta\varepsilon_F)\beta_e/4]}{\cosh[(2\varepsilon_F-\varepsilon+\Delta\varepsilon_F)\beta_e/4]}+\frac{\xi-\Delta\varepsilon_F}{2}\beta_e\right\}, \tag{15}$$

$$F(y)=\sinh\left(\frac{y}{2}\right)\left[\frac{35}{4}I_1(y)-I_3(y)\right]+I_2(y)\cosh\left(\frac{y}{2}\right). \tag{16}$$

The function W depends on the Fermi energy:

$$\varepsilon_F=\beta_e^{-1}\ln\left\{\sqrt{\cosh^2\left[\frac{(\varepsilon-\Delta\varepsilon_F)\beta_e}{2}\right]+\exp\left(\frac{2\pi\hbar^2 n_e\beta_e}{m_e}\right)-1}-\cosh\left[\frac{(\varepsilon-\Delta\varepsilon_F)\beta_e}{2}\right]\right\}. \tag{17}$$

$I_n=\langle M^n\rangle$ is proportional to the nth derivative of the statistical sum of Mn states Z:

$$I_n(y)=\sum_{M=-5/2}^{5/2} M^n\frac{N_M}{N}=(-1)^n\frac{1}{Z(y)}\frac{d^n}{dy^n}Z(y). \tag{18}$$

In the presence of the field an electron with spin projection m has an energy

$$\varepsilon_m=-\delta_e N_0\alpha x_{\mathrm{Mn}} m\langle S_z\rangle+m g_e^*\mu_B B,\quad m=\pm\frac{1}{2}, \tag{19}$$

where the first part is the exchange energy in the frame of the virtual-crystal and molecular-field approximations, with the thermal mean value of the Mn spin $\langle S_z\rangle$ defined in Eq. (2). The second part is the Zeeman term with the intrinsic electron g factor g_e^*. If the system deviates slightly from thermodynamic equilibrium ($\Theta_e\approx\Theta_{\mathrm{Mn}}$, $\Delta\varepsilon_F\approx 0$), Eq. (13) is zero, and the energy flux from the electron gas to the magnetic ion system vanishes. For small deviations from the equilibrium [$\sinh x\approx x$ in Eq. (13)] the product WF represents the electron-Mn relaxation rate, and from Eqs. (6) and (13) we obtain

$$\frac{T_{\mathrm{SL}}}{T_{e\text{-Mn}}}\left(\beta_e-\beta_{\mathrm{Mn}}-\beta_e\frac{\Delta\varepsilon_F}{\xi}\right)=\beta_{\mathrm{Mn}}-\beta_L. \tag{20}$$

Hence for small differences between the electron temperature and the lattice temperature the basic parameter of our theory is the ratio $T_{\mathrm{SL}}/T_{e\text{-Mn}}$. If $T_{e\text{-Mn}}\gg T_{\mathrm{SL}}$ the temperature of the magnetic ions is equal to the lattice temperature. In the opposite limit, Θ_{Mn} is determined by the interaction with the 2DEG. Generally, $T_{e\text{-Mn}}$ depends strongly on the temperatures of the 2DEG and of the magnetic ion system, and on the splitting of the electron quasi Fermi levels. These dependencies can be neglected if $\Theta_e\approx\Theta_{\mathrm{Mn}}\approx\Theta_L$ and $\Delta\varepsilon_F\approx 0$. For such a case $T_{e\text{-Mn}}$ is drawn in Fig. 10 as a function of the magnetic field for various electron concentrations, $\Theta_{\mathrm{Mn}}\approx\Theta_L=2$ K and $x_{\mathrm{Mn}}=0.01$. Further parameters are $m_e=0.096m_0$, $L=80$ Å, $\alpha=1.5\times10^{-29}$ eV m^3, and $g_e^*=-1.46$. In the absence of a magnetic field, $T_{e\text{-Mn}}$ decreases with increasing electron concentration if the electron gas is nondegenerate. For a degenerate electron gas (for values of n_e chosen in Fig. 10, this is valid in the range $n_e\geqslant 5\times10^{10}$ cm^{-2}) $T_{e\text{-Mn}}$ does not depend on n_e. The field dependence of the electron-magnetic ion relaxation time becomes less pronounced for higher electron concentrations.

Another factor, apart from the electron density and temperature, that determines the degree of Mn heating is the concentration of magnetic ions. As the spin-lattice relaxation time shortens with the formation of ion clusters, the heating is unlikely to show up in samples with high Mn fractions, where $T_{e\text{-Mn}}>T_{\mathrm{SL}}$. Moreover, the spin-flip process itself depends on x_{Mn} via the electron spin splitting. In Fig. 10 the spin-lattice relaxation time T_{SL} calculated with experimental values of τ_{SL} taken from Ref. 12 ($x_{\mathrm{Mn}}=0.01$) is presented by a thick solid curve. For an electron density $n_e\approx10^{10}$ cm^{-2} $T_{e\text{-Mn}}$ is about eight times shorter than the spin-lattice relaxation time T_{SL} at $B=0$, and longer than T_{SL} in the presence of the field $B>0.3$ T. The region of magnetic fields where the condition $T_{e\text{-Mn}}<T_{\mathrm{SL}}$ is valid, and where heating of the Mn system should occur, increases with n_e. For electron

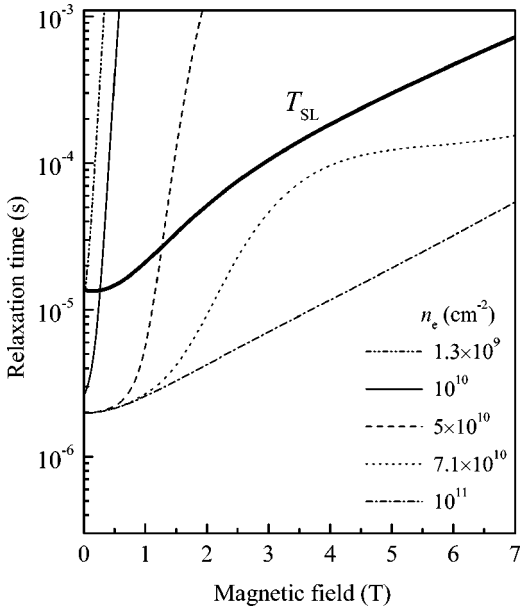

FIG. 10. Magnetic-field dependence of the electron-magnetic ion relaxation time $T_{e\text{-Mn}}$ for different electron concentrations and $x_{\mathrm{Mn}}=0.01$ determined by Eq. (14). T_{SL} is a modified spin relaxation time as defined in Sec. V, with the field dependence of τ_{SL} taken from Ref. 12. The following parameters were used: $m_e=0.096m_0$, $L=80$ Å, $\alpha=1.5\times10^{-29}$ eV m^3, and $g_e^*=-1.46$.

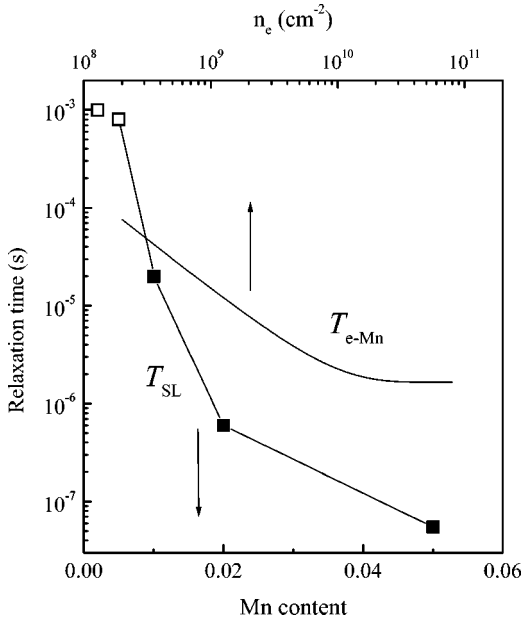

FIG. 11. Calculated electron-Mn relaxation time $T_{e\text{-Mn}}$ as a function of the 2DEG concentration (upper scale) for $B\rightarrow 0$. The same parameters were used as for the calculations shown in Fig. 10. Symbols represent values for the spin-lattice relaxation time T_{SL} as a function of the Mn mole fraction (lower scale), deduced with τ_{SL} taken from Refs. 46 (open symbols) and 12 (closed symbols).

concentrations above 8×10^{10} cm^{-2} the condition $T_{e\text{-Mn}}<T_{\mathrm{SL}}$ is satisfied for the whole range of magnetic fields studied. Figure 11 compares $T_{e\text{-Mn}}$ as a function of the 2DEG concentration in the limit $B\rightarrow 0$, with T_{SL} for various Mn contents. As mentioned above, the relaxation time $T_{e\text{-Mn}}$ saturates for high electron concentrations, where the 2DEG is degenerate. The figure can be used to determine the condition for which heating of the Mn system can be observed. That is for $x_{\mathrm{Mn}}=0.01$ the Mn system is significantly influenced by the 2DEG for concentrations larger than $\approx 10^9$ cm^{-2} only, where $T_{e\text{-Mn}}<T_{\mathrm{SL}}$. Already for $x_{\mathrm{Mn}}>0.016$, $T_{e\text{-Mn}}$ is longer than T_{SL} even for the highest electron concentrations. Note that $T_{e\text{-Mn}}$ depends on the electron mass, QW width, and exchange constant, the factors which allow one to control the conditions, and thus the degree, of the Mn heating.

In semimagnetic semiconductors the electron system is usually characterized by short times of the spin relaxation. Therefore, effects of optical orientation by photocarriers can often be ignored. However, in the present case, the electron-Mn spin-flip transitions not only heat the Mn system but, at the same time, create a nonequilibrium electron polarization, i.e., they lead to an increase of the difference between the quasi-Fermi levels of the two electron spin-split subbands $\Delta\varepsilon_F$. For very short spin relaxation times of electrons τ_s, the equilibrium population of the electron spin states is established very quickly and one can neglect $\Delta\varepsilon_F$ in Eq. (20). Then only the electron temperature determines the Mn heating. In the opposite case the electron-spin state $m_s=1/2$ will be depopulated by the spin-flip scattering (increase of $\Delta\varepsilon_F$), which decreases the number of scattering events that heat the Mn system. Here one has to account for the spin flux to the electron system due to exchange scattering with Mn ions, and also due to an intrinsic electron spin relaxation time τ_s. For diamondlike semiconductors we have $10^{-10}<\tau_s<10^{-8}$ s.[38]

The spin-flip transition generates a difference between the population n_m of spin-up and -down subbands with a velocity

$$\frac{\partial(n_{+1/2}-n_{-1/2})}{\partial t}=-\frac{2}{\xi}\left.\frac{\partial E}{\partial t}\right|_{e\text{-Mn}}. \tag{21}$$

The temporal change of $\Delta\varepsilon_F$ is

$$\frac{d\Delta\varepsilon_F}{dt}=-\frac{\Delta\varepsilon_F}{\tau_s}-\frac{\partial\Delta\varepsilon_F}{\partial(n_{+1/2}-n_{-1/2})}\frac{2}{\xi}\left.\frac{\partial E}{\partial t}\right|_{e\text{-Mn}}. \tag{22}$$

Taking Eqs. (6) and (13) into account, one can write the final system of nonlinear equations for the Mn spin temperature and Fermi-level splitting in the form

$$\beta_e\Delta\varepsilon_F=\frac{T_s}{T_{\mathrm{SL}}}\xi(\beta_{\mathrm{Mn}}-\beta_L), \tag{23}$$

$$\xi(\beta_e-\beta_{\mathrm{Mn}})=\frac{T_{e\text{-Mn}}+T_s}{T_s}\beta_e\Delta\varepsilon_F, \tag{24}$$

$$T_s=\tau_s\frac{16\pi x_{\mathrm{Mn}}N_0\hbar^2L\beta_e}{m_e\{2+\tanh[(2\varepsilon_F-\varepsilon+\Delta\varepsilon_F)\beta_e/4]+\tanh[(2\varepsilon_F+\varepsilon-\Delta\varepsilon_F)\beta_e/4]\}}. \tag{25}$$

If the difference between magnetic ion and lattice temperature is small, i.e., $I_1(\xi\beta_L)-I_1(\xi\beta_{\mathrm{Mn}})\approx\xi[I_2(\xi\beta_{\mathrm{Mn}})-I_1^2(\xi\beta_{\mathrm{Mn}})](\beta_{\mathrm{Mn}}-\beta_L)$, one can use $\beta_e\approx\beta_{\mathrm{Mn}}\approx\beta_L$ and $\Delta\varepsilon_F\approx 0$. In this limit Eqs. (23) and (24) is a system of linear equations resulting in

$$\beta_{\mathrm{Mn}}-\beta_L=\frac{T_{\mathrm{SL}}}{T_{\mathrm{SL}}+(T_{e\text{-Mn}}+T_s)}(\beta_e-\beta_L). \tag{26}$$

It follows from Eq. (26) that the heating of the Mn spin system is determined by the ratio $T_{\mathrm{SL}}/(T_{e\text{-Mn}}+T_s)$, where $T_{e\text{-Mn}}+T_s$ is the total characteristic time of energy transfer from the 2DEG into the Mn spin system. In Fig. 12 the field dependences of T_s, $T_{e\text{-Mn}}$, and T_{SL} are presented for $x_{\mathrm{Mn}}=0.01$ using the following parameters: $n_e=3\times 10^{10}$ cm^{-2}, $\Theta_L=2$ K, $\tau_s=0.1$ ns, and $N_0=1.47\times 10^{22}$ cm^{-3}. All other parameters are given in the caption of Fig. 10. One can

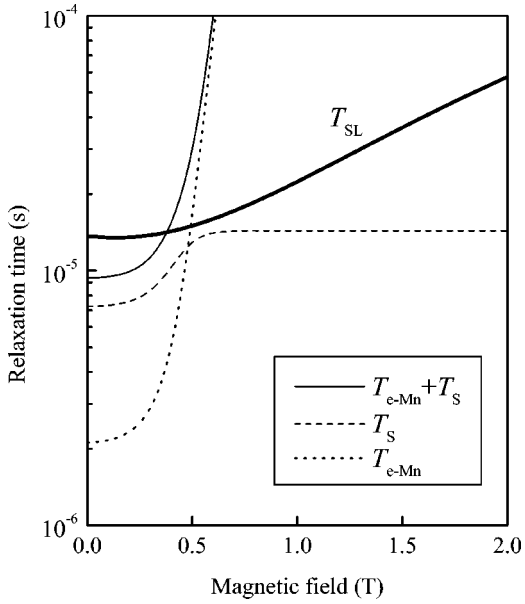

FIG. 12. Theoretical relaxation times $T_{e\text{-Mn}}$ [Eq. (14)] and T_s [Eq. (25)] for $x_{\mathrm{Mn}}=0.01$, $\Theta_L=2$ K, and $n_e=4\times10^{10}$ cm^{-2} as a function of magnetic field. T_{SL} is a modified spin-relaxation time as defined in Sec. V, with the field dependence of τ_{SL} taken from Ref. 12. The same parameters were used as for the calculations shown in Fig. 10, and $N_0=1.47\times10^{22}$ cm^{-3}.

see that for small magnetic fields $B<0.5$ T the time of electron-magnetic ion energy transfer is dominated by T_s, which is considerably longer than $T_{e\text{-Mn}}$. As a result the splitting of the Fermi level (i.e., nonequilibrium electron-spin polarization) suppresses the heating of the Mn spin system here. In the high-field regime $B>0.5$ T, the electron-Mn interaction is determined by $T_{e\text{-Mn}}(>T_s)$, and the Fermi-level splitting does not influence the Mn spin temperature.

The calculation done is restricted to isolated Mn ions which is justified for DMS's with a few percent of Mn mole fraction and sufficient for the studied structure. That is, for $x_{\mathrm{Mn}}=0.01$ the probability of finding isolated ions with no nearest neighbors is 90% (after Ref. 39). For higher Mn compositions the probability for isolated Mn ions is reduced (e.g., 50% for $x_{\mathrm{Mn}}=0.05$) which would require a treatment of Mn ions coupled in clusters (pairs, triplets) via the superexchange interaction. In Sec. VI we compare results of our model with experimental values of Θ_{Mn}.

VI. DISCUSSION

The linear approach for the Mn temperature given in Sec. V is valid only for small deviations from the thermodynamic equilibrium ($\Theta_{\mathrm{Mn}}\approx\Theta_L$). In experiments, however, the Mn temperature increases up to 8 K. Therefore, we have to analyze the experimetnal data by numerical solutions of the coupled nonlinear equations (23) and (24). In addition to the parameters already given in Sec. III, we used the electron effective mass $m_e=0.096m_0$,[40] the electron-spin relaxation time $\tau_s=0.1$ ns, and the field-dependent spin-lattice relaxation time τ_{SL} taken from data of Ref. 12 [τ_{SL} covers the range $\approx4\times10^{-5}$ s ($B=0$) up to $\approx4\times10^{-6}$ s ($B=9$ T)]. The value of τ_s is of the same order of magnitude as determined in GaAs-based QW's.[32] The intrinsic electron g factor in CdTe-based QW's was determined in Ref. 41, and is $g_e^*=-1.46$ in the studied structure, where the energy of the heavy-hole exciton transition is 1.65 eV. The electron density, which influences the Mn heating according to Eq. (17), changes for excitation above the barrier band gap (see Fig. 3). For this reason we have interpolated n_e for the individual excitation densities between the values determined from the reflectivity spectra, assuming a linear increase of n_e with P_L. The electron densities used in our calculation are listed in Table I. Our best fits to the field-dependent Mn temperature for different excitation powers are plotted by solid curves in Fig. 7. We restricted the calculations to magnetic fields lower than 4 T, as we did not take Landau quantization into account, which may be of importance for high-field values. The X^- energies determined by Eq. (1) with the field-dependent Mn temperature are shown in Fig. 6 by solid lines. Especially for the two lowest excitation densities the agreement between experiment and theory is quite good. However, there are significant deviations from the experimental data for higher excitation densities.

Although the field dependence of Θ_{Mn} cannot be simulated for all excitation densities with high precision, we can estimate the electron temperature Θ_e from the limit $B\rightarrow0$. The dependence of Θ_e on the excitation power density P_L evaluated from the best fit is plotted in the inset of Fig. 7 by solid symbols. The electron temperature reveals a reasonable monotonic increase with P_L. It is possible to reproduce the overall behavior of Θ_{Mn} for the two lowest excitation densities using a lattice temperature of $\Theta_L=1.6$ K (the temperature of the He bath). However for $\Theta_L=1.6$ K we found differences between theoretical and experimental points in the field range where Θ_{Mn} saturates. Thus we additionally adjusted the lattice temperature in addition to the electron temperature. The best agreement between experiment and theory was obtained for $\Theta_L\approx2.3$ K. We assume that this small heating of the lattice is generated by direct interaction of the lattice either with the 2DEG or with the magnetic system, i.e., the spin-lattice relaxation. Further studies are required to clarify this small increase of the lattice temperature.

According to the Fermi energy [see Eq. (17)], which contributes to the energy flux $\partial E/\partial t$ the Mn overheating depends on the concentration of the 2DEG. This relation was shown experimentally in Sec. III by the different energy shift of the X^- luminescence line for below- and above-barrier excitation (see the inset of Fig. 8). For completeness we have calculated the trion energy as a function of B for the case of a fixed electron density $n_e=1.2\times10^{10}$ cm^{-2}, which corresponds to experimental conditions of below-barrier excitation. Equations (1), (23), and (24) were used, with $\Theta_e=8.7$ K, $\Theta_L=1.9$ K, and $\tau_s=0.1$ ns (further values are given above). The calculated values are shown by a dotted line in Fig. 8; they quantitatively reproduce the experimental points.

Let us summarize the results of the fitting procedure. We found that the theory describes well the value of the Mn-system heating in the whole range of magnetic fields in the case of low levels of photoexcitation. In fact, we have used one basic fitting parameter: the temperature of the 2DEG Θ_e. Another parameter—the electron-spin relaxation time τ_s

without contribution of the flipflop scattering by magnetic ions—can be tuned in a wide range. However, this time cannot be longer than the spin-relaxation time of the electrons via the flipflop process with Mn ions $\tau_{\text{flipflop}} = 8\hbar^3 L/15\alpha^2 m_e N_0 x_{\text{Mn}} \approx 6\times 10^{-11}$ s, i.e. $\tau_s \leqslant \tau_{\text{flipflop}} \approx 10^{-10}$ s. In the case $\tau_s > \tau_{\text{flipflop}}$ a large nonequilibrium polarization of the 2DEG would develop, and this would prevent the heating of the Mn system. An electron-spin relaxation time of the order 10^{-10} s is consistent with values found in the literature (e.g., Ref. 33). Typical spin-relaxation times in nonmagnetic semiconductors cover the range from 10^{-10} up to 10^{-8} s.[38] They are usually related to the following relaxation mechanisms: Elliot-Yaffet,[42] D'yakonov-Perel',[43] and Bir-Aronov-Pikus (BAP).[44] It is not clear which of these mechanisms dominates in our structures. However, we can suggest that under low levels of photoexcitation the concentration of the photoholes is small, and that the BAP mechanism does not play an important role.

It is worthwhile to note that in the case $\tau_s \approx 10^{-10}$ s a remarkable nonequilibrium polarization of the 2DEG caused by flipflop scattering can be achieved, and that the splitting between quasi-Fermi levels for different spin orientations reaches several hundreds of μeV. It is important to note that this polarization is caused by interaction with the magnetic ions, and that its value increases with an increasing concentration of magnetic ions. This is contrary to the optical orientation effect,[11] which is suppressed by increasing Mn content (due to acceleration of the spin-lattice relaxation processes). In the case of high levels of photoexcitation, when the 2DEG temperature elevates to 10 K and the electron concentrations increase a few times, our model does not satisfactory describe the decrease of the Mn-ion temperature in magnetic fields stronger than 1 T. Under these conditions the suppression of the flipflop processes in the magnetic fields is not very effective; the calculated time of $T_{e\text{-Mn}}$ is always shorter than T_{SL}, and the theoretical value for the Mn-spin temperature significantly exceeds the experimental data. Several explanations for his deviation can be suggested. (i) The Landau quantization of the electron spectrum in high fields should reduce the probability of the flipflop transitions. In the limit of unbroadened Landau levels, the energy conservation law requires that the energy distance between Landau levels is equal to the sum of the Zeeman energy of the electron in the exchange field and the Zeeman energy of the Mn spin in the external field. (ii) The suppression of the intrinsic spin-relaxation time of the electrons with increasing magnetic fields, i.e., the increase of τ_s, will also lead to a decrease of the heating efficiency. In the frame of the D'yakonov Perel' mechanism this field dependence can be expressed by $\tau_s(B) = \tau_s(0)(1 + B^2/B_0^2)$.[38] Applying this formula to Eq. (25) with the parameters $\tau_s(0) = 10^{-10}$ s and $B_0 = 1$ T, we have calculated values of the Mn temperature, as shown by dotted curves in Fig. 7. The values of Θ_e extracted for $\tau_s(B)$ are shown by open symbols in Fig. 7. Obviously the agreement between experiment and theory is improved. However, a detailed theoretical analysis of the heating in high magnetic fields requires a refinement of the model employed, and is beyond the scope of this paper.

Finally, we note that for a 2DEG concentration smaller than 10^{10} cm^{-2} the time $T_{e\text{-Mn}}$ increases strongly, and the range of magnetic fields where $T_{e\text{-Mn}} < T_{\text{SL}}$ decreases. For $n_e < 10^9$ cm^{-2} and $\Theta_e = 2$ K the condition $T_s > T_{\text{SL}}$ is valid for all values of magnetic fields, and the heating of the Mn system is practically absent. A sizable heating of the Mn system in this case is possible if the photoexcitation provides not only a heating of the 2DEG, but also a significant increase of the concentration of the 2DEG.

In conclusion, we have experimentally found an efficient channel of energy transfer from photocarriers into the Mn system via a 2DEG. An *n*-type modulation-doped $Cd_{0.99}Mn_{0.01}Te/Cd_{0.76}Mg_{0.24}Te$ quantum well was investigated by reflectance and photoluminescence in external magnetic fields. We suggested a model of the energy exchange between the 2DEG and the Mn system which allowed us to obtain a good quantitative description with the experimental data. The presented mechanism is based on the spin-flip scattering of electrons on magnetic ions and, thus, depends on the magnetic-field value. Our studies may be of importance for the research of spintronic devices, where a current of electrons is spin polarized in an *n*-type doped semimagnetic semiconductor.[45]

ACKNOWLEDGMENTS

This work was supported by the Deutsche Forschungsgemeinschaft through Sonderforschungsbereich 410. The work in Poland was supported by a grant from the State Committee for Scientific Research under Contract No. PBZ-28.11. S.M. R.'s visit in Würzburg was supported by NATO Grant No. HTECH.EV 974696.

[1] J.K. Furdyna, J. Appl. Phys. **64**, R29 (1988).
[2] J. Kossut and W. Dobrowolski, in *Handbook of Magnetic Materials*, edited by K.H.J. Buschow (Elsevier, Amsterdam, 1993), Vol. 7, p. 231.
[3] D.R. Yakovlev and K.V. Kavokin, Comments Condens. Matter Phys. **18**, 51 (1996).
[4] M.G. Tyazhlov, V.D. Kulakovskii, A.I. Filin, D.R. Yakovlev, A. Waag, and G. Landwehr, Phys. Rev. B **59**, 2050 (1999).
[5] M.G. Tyazhlov, A.I. Filin, A.V. Larionov, V.D. Kulakovskiĭ, D.R. Yakovlev, A. Waag, and G. Landwehr, Zh. Éksp. Teor. Fiz. **112**, 1440 (1997) [JETP **85**, 784 (1997)].
[6] V.D. Kulakovskii, M.G. Tyazhlov, A.I. Filin, D.R. Yakovlev, A. Waag, and G. Landwehr, Phys. Rev. B **54**, R8333 (1996).
[7] S.M. Ryabchenko, Yu.G. Semenov, and O.V. Terletskiĭ, Zh. Éksp. Teor. Fiz. **82**, 951 (1982) [Sov. Phys. JETP **55**, 557 (1982)].
[8] H. Krenn, W. Zawadzki, and G. Bauer, Phys. Rev. Lett. **55**, 1510 (1985).
[9] D.D. Awschalom, J. Warnock, and S. von Molnár, Phys. Rev. Lett. **58**, 812 (1987).
[10] H. Krenn, K. Kaltenegger, T. Dietl, J. Spałek, and G. Bauer, Phys. Rev. B **39**, 10 918 (1989).
[11] Yu.G. Semenov, Zh. Éksp. Teor. Fiz. **81**, 1498 (1981) [Sov. Phys. JETP **54**, 794 (1981)].

[12] T. Strutz, A.M. Witowski, and P. Wyder, Phys. Rev. Lett. **68**, 3912 (1992).
[13] D. Scalbert, J. Cernogora, and C. Benoit a la Guillaume, Solid State Commun. **66**, 571 (1988).
[14] J. Shah, *Hot Carriers in Semiconductor Nanostructures: Physics and Applications* (Academic Press, San Diego, 1992).
[15] B.M. Ashkinadze, A. Nazimov, E. Cohen, A. Ron, and L.N. Pfeiffer, in *Proceedings of the 24th International Conference on the Physics of Semiconductors*, edited by D. Gershoni (World Scientific, Singapore, 1998).
[16] T. Wojtowicz, M. Kutrowski, G. Karczewski, and J. Kossut, Appl. Phys. Lett. **73**, 1379 (1998).
[17] B. Kuhn-Heinrich, W. Ossau, E. Bangert, A. Waag, and G. Landwehr, Solid State Commun. **91**, 413 (1994).
[18] D.R. Yakovlev, V.P. Kochereshko, R.A. Suris, H. Schenk, W. Ossau, A. Waag, G. Landwehr, P.C.M. Christianen, and J.C. Maan, Phys. Rev. Lett. **79**, 3974 (1997).
[19] K. Kheng, R.T. Cox, Y. Merle d'Aubigné, F. Bassani, K. Saminadayar, and S. Tatarenko, Phys. Rev. Lett. **71**, 1752 (1993).
[20] T. Dietl, A. Haury, and Y. Merle d'Aubigné, Phys. Rev. B **55**, R3347 (1997).
[21] A. Haury, A. Wasiela, A. Arnoult, J. Cibert, S. Tatarenko, T. Dietl, and Y. Merle d'Aubigné, Phys. Rev. Lett. **79**, 511 (1997).
[22] B. König, U. Zehnder, D.R. Yakovlev, W. Ossau, T. Gerhard, M. Keim, A. Waag, and G. Landwehr, Phys. Rev. B **60**, 2653 (1999).
[23] K. Chern-Yu, W.C. Chou, A. Twardowski, W.Y. Yu, S.T. Lee, A. Petrou, J. Warnock, and B.T. Jonker, J. Appl. Phys. **75**, 2988 (1994).
[24] W. Ossau, D.R. Yakovlev, G. Astakhov, V.P. Kochereshko, J. Nürnberger, W. Faschinger, and G. Landwehr, Physica E (Amsterdam) **6**, 187 (2000).
[25] G. Astakhov, D.R. Yakovlev, V.P. Kochereshko, W. Ossau, J. Nürnberger, W. Faschinger, and G. Landwehr, Phys. Rev. B **60**, R8485 (1999).
[26] V.P. Kochereshko, D.R. Yakovlev, A.V. Platonov, W. Ossau, A. Waag, G. Landwehr, and R.T. Cox, in *Proceedings of the 23rd International Conference on Physics of Semiconductors*, edited by M. Scheffler and R. Zimmermann (World Scientific, Singapore, 1996), p. 1943.
[27] D. Heiman, P. Becla, R. Kershaw, D. Ridgley, K. Dwight, A. Wold, and R.R. Galazka, Phys. Rev. B **34**, 3961 (1986).
[28] J.A. Gaj, R. Planel, and G. Fishman, Solid State Commun. **29**, 435 (1979).
[29] W. Ossau, R. Fiederling, B. König, T. Wojtowicz, M. Kutrowski, G. Karczewski, and J. Kossut, Phys. Low-Dimens. Semicond. Struct. **11/12**, 89 (1997).
[30] W.J. Ossau and B. Kuhn-Heinrich, Physica B **184**, 422 (1993).
[31] J. Shah, Solid-State Electron. **21**, 43 (1978).
[32] T.C. Damen, L. Viña, J.E. Cunningham, J. Shah, and L.J. Sham, Phys. Rev. Lett. **67**, 3432 (1991).
[33] M.Z. Maialle, E.A. de Andrada e Silva, and L.J. Sham, Phys. Rev. B **47**, 15 776 (1993).
[34] B.L. Gelmont, V.I. Ivanov-Omskii, and E.I. Tsidilkovski, Semicond. Sci. Technol. **5**, S281 (1990).
[35] R. Ferreira and G. Bastard, Phys. Rev. B **43**, 9687 (1991).
[36] G. Bastard and L.L. Chang, Phys. Rev. B **41**, 7899 (1990).
[37] J. Kossut, Phys. Status Solidi B **72**, 359 (1975).
[38] G. Pikus and A.N. Titkov, in *Optical Orientation*, edited by F. Meier and B.P. Zakharchenya (North-Holland, Amsterdam, 1984), Vol. 8, p. 73.
[39] Y. Shapira, S. Foner, D.H. Ridgley, K. Dwight, and A. Wold, Phys. Rev. B **30**, 4021 (1984).
[40] P. Lawaetz, Phys. Rev. B **4**, 3460 (1971).
[41] A.A. Sirenko, T. Ruf, M. Cardona, D.R. Yakovlev, W. Ossau, A. Waag, and G. Landwehr, Phys. Rev. B **56**, 2114 (1997).
[42] Y. Yaffet, in *Solid State Physics*, edited by F. Seitz and D. Turnbull (Academic Press, New York, 1963), Vol. 14, p. 1.
[43] M.I. D'yakonov and V.I. Perel', Zh. Éksp. Teor Fiz. **60**, 1954 (1971) [Sov. Phys. JETP **33**, 1054 (1971)].
[44] G.L. Bir, A.G. Aronov, and G.E. Pikus, Zh. Éksp. Teor Fiz. **69**, 1382 (1975) [Sov. Phys. JETP **42**, 705 (1976)].
[45] R. Fiederling, M. Keim, G. Reuscher, W. Ossau, G. Schmidt, A. Waag, and L.W. Molenkamp, Nature (London) **402**, 787 (1999).
[46] D. Scalbert, Phys. Status Solidi B **193**, 189 (1996).